Chirped pulse excitation in condensed phases involving intramolecular modes studied by double-sided Feynman diagrams for fast optical dephasing

B. D. Fainberg[a] and V. Narbaev
Holon Academic Institute of Technology, Department of Exact Sciences, 52 Golomb Street, Holon 58102, Israel and Raymond and Beverly Sackler Faculty of Exact Sciences, School of Chemistry, Tel-Aviv University, Tel-Aviv 69978, Israel

(Received 12 June 2000; accepted 16 August 2000)

The effect of the quantum intramolecular modes on the chirped pulse excitation in condensed phase has been studied. Nonperturbative equations for the populations of molecular electronic states under the action of intense chirped pulses have been obtained using the double-sided Feynman diagrams. We have shown that the application of this technique to systems with fast electronic dephasing enables us to include strong system–bath interactions (non-Markovian relaxation) and to perform the summation of diagrams. We have studied the influence of the chirp rate on the integral population of the excited state n_2 after the completion of pulse action. We have shown that the effect of the quantum intramolecular modes strongly depends on the carrier pulse frequency. Incorporating these modes increases n_2 when a molecule is excited near the $0\rightarrow 1$ transition with respect to the quantum intramolecular vibration. If the molecule is excited near the $0\rightarrow 0$ transition with respect to the intramolecular mode, the effect is opposite. © *2000 American Institute of Physics.* [S0021-9606(00)52142-4]

I. INTRODUCTION

Recent experiments on optical control have involved the use of chirped pulses.[1–16] The phase structure (chirp) of the pulse determines the temporal ordering of its different frequency components that enables us to control molecular dynamics.[17] In particular, chirped pulses can selectively excite coherent wave packet motion either on the ground electronic potential-energy surface of a molecule or on the excited electronic potential surface.[8,14] This property of chirped pulses can be essentially enhanced by going beyond the perturbative regime due to the multiphoton processes of exciting molecules.[13]

The effects of varying the chirp and intensity of an ultrashort pulse exciting dye molecules in liquid solutions have been investigated experimentally by Shank *et al.*,[13] Bardeen, Wilson *et al.*,[15] and Huppert *et al.*[16] They measured the integrated fluorescence (which is directly proportional to the integral excited state population) after the completion of the pulse action, as a function of pulse chirp. In addition, Shank *et al.*[13] and Huppert *et al.*[16] measured the absorption spectrum of chirped pulses. For low-power excitation, they found that the absorption and amount of excited state population were independent of chirp, while for high-power excitation the authors[13,15,16] observed a strong chirp dependence.

The interaction of strong radiation (and especially intense chirped pulses) with large molecules in solutions is rather a complex problem. This problem involves two types of nonperturbative interactions: light-matter and relaxation (non-Markovian) ones.[18,19] Therefore, the majority of nonperturbative light-matter descriptions was carried out by numerical solving the corresponding sets of equations for molecular systems noncoupled[4,13,20,21] and coupled[22,23] with a dissipative environment.

In Ref. 24 a nonperturbative analytic approach to the problem of the interaction of high-power chirped ultrashort pulses with molecular systems has been developed: The picture of ''moving potentials.'' We have considered a strongly broadened vibronic system of low-frequency (LF) optically active (OA) intra- and intermolecular vibrations $\{\omega_s\}$ with dissipation interacting with a strong chirped pulse. Its field amplitude can be represented in the form

$$\boldsymbol{E}(t)=\boldsymbol{\mathcal{E}}(t)\exp(i\varphi(t)), \tag{1}$$

where $\mathcal{E}(t)$ and $\varphi(t)$ are real functions of time, and $\varphi(t)$ describes the change of the pulse phase in a time t. The solution of the problem was based on the following facts:

(1) The irreversible dephasing time of the electronic transition T' for such a system is much shorter than both the vibrational relaxation time τ_s and pulse duration t_p;
(2) the pulse frequency $\omega(t)=\omega-d\varphi/dt$ changes only slightly during T';
(3) relaxation of the vibrational excitation in the ground and excited electronic states can be described as diffusion with respect to the energetic coordinate.

The approximation of fast electronic dephasing was used also in a simplified approach to the problem under consideration: Time-dependent rate equations, developed by Bardeen *et al.*[25]

Theory[24] naturally leads to the picture of ''moving'' potentials which are ''photonic replications'' of the ground and excited electronic states. An electronic optical transition in-

[a]Electronic mail: fainberg@barley.cteh.ac.il

duced by chirped pulses, can be considered as an electron transfer reaction between a ''moving photonic replication'' and the corresponding term occurring at their instantaneous intersection. In Ref. 26 the approach[24] has been generalized to different relaxation times in electronic states 1 and 2.

However, the absorption spectrum of large molecules in solutions shows a progression with respect to a high-frequency (HF) OA vibration ($\approx 1000\ \mathrm{cm}^{-1}$) (see inset to Fig. 9). Each member of this progression is broadened due to the presence of LFOA intra- and intermolecular vibrations $\{\omega_s\}$. Thus, one can consider an absorption spectrum of a large molecule in solution as consisting from overlapping vibronic transitions. Our previous considerations[24,26] concerned only one vibronic transition. This can be a reasonable approximation to L690 in solution used in experiments by Shank *et al.*[13] since its absorption spectrum shows the main maximum corresponding to $0 \rightarrow 0$ transition with respect to a HFOA vibration, and the remaining have much less intensities.[27] However, the molecule LDS750 used in experiments by Shank *et al.*, and many others do not correspond to this model. Therefore, we need to generalize our consideration to the presence of a number of vibronic transitions. We intend to study the effect of HF intramolecular modes on the excited-state population n_2 as a function of chirp rate.

A strong analogy exists between optical transitions in strong fields and electron transfer reactions under strong interaction (solvent-controlled limit).[18,19,24,26,28] The influence of intramolecular vibrational excitations on the solvent-controlled electron transfer reactions was investigated in Refs. 29 and 30. It has been shown that the presence of high-frequency quantum modes gives rise to parallel vibronic channels, each involving a distinct intramolecular vibrational excitation of the initial and final states.

A similar effect will be in the case of a molecular system interacting with a strong phase modulated pulse where the only difference is that the parallel vibronic channels will be related to a number of intersections of photonic replications and vibronic terms.

However, it is not evident that the solution of the problem will be a direct generalization of our approach.[24] The point is that one must take into account the interference effects which are similar to the interference of different channels in the electron transfer reactions.[31] These effects are of considerable significance for the ''inverted region'' according to Marcus theory of the (free) energy gap (ΔE) law.[32–35] In the photon replica picture,[19,24,26,28] the frequency detuning $\hbar\Delta\omega(t) \equiv \hbar[\omega(t) - \omega_{21}^{\mathrm{el}}]$ (between instantaneous pulse frequency and the frequency of purely electronic transition $1 \rightarrow 2$ $\omega_{21}^{\mathrm{el}}$) plays the role of ΔE for the optical transitions in the field of strong chirped pulses, i.e., $\Delta E(t) = \hbar[\omega(t) - \omega_{21}^{\mathrm{el}}]$. Therefore, one can realize all the Marcus regions in one experiment with chirped pulses: the ''normal region,'' the ''activationless region'' and the inverted region.

In this work the problem under consideration is solved using the double-sided Feynman diagrams.[36–38] We show that the application of the double-sided Feynman diagrams to systems with fast electronic dephasing opens up new possibilities for using this technique in resonance nonlinear optical spectroscopy. The novel potentials are including strong system–bath interactions (non-Markovian relaxation) and the summation of diagrams. The last procedures enable us to obtain nonperturbative equations for the populations of molecular electronic states under the action of intense chirped pulses in the presence of hf quantum modes (see Sec. II). Some of the preliminary results on the double-sided Feynman diagrams in the fast electronic dephasing limit, not including the excitation of intramolecular quantum modes, are presented in Conference Proceedings.[39] In Sec. II we give a full account of this study with new results related to the presence of intramolecular quantum modes.

The remainder of this paper is organized as follows. In Sec. III we use the obtained equations to study the effect of quantum intramolecular modes on the chirped pulse excitation of molecules in solutions. In Sec. IV we summarize our results.

II. DERIVATION OF EQUATIONS FOR POPULATIONS OF ELECTRONIC STATES UNDER THE ACTION OF CHIRPED PULSE

Let us consider a molecule with two electronic states $n = 1$ and 2 in a solvent described by the Hamiltonian

$$H_0 = \sum_{n=1}^{2} |n\rangle [E_n + W_n(\mathbf{Q})] \langle n|, \tag{2}$$

where $E_2 > E_1$, E_n is the energy of state n, $W_n(\mathbf{Q})$ is the adiabatic Hamiltonian of reservoir R (the vibrational subsystems of a molecule and a solvent interacting with the two-level electron system under consideration in state n). The molecule is affected by electromagnetic radiation of frequency ω

$$\mathbf{E}(t) = \tfrac{1}{2}\boldsymbol{E}(t)\exp(-i\omega t) + \text{c.c.} \tag{3}$$

For phase modulated pulses the field amplitude $\boldsymbol{E}(t)$ can be presented by Eq. (1).

Since an absorption spectrum of a large molecule in solution consists from overlapping vibronic transitions, we shall single out the contribution from LFOA vibrations $\{\omega_s\}$ to $W_n(\mathbf{Q})$: $W_n(\mathbf{Q}) = W_{nM} + W_{ns}$ where W_{ns} is the sum of the Hamiltonian governing the nuclear degrees of freedom of the solvent in the absence of the solute and LFOA intramolecular vibrations, and the part which describes interactions between the solute and the nuclear degrees of freedom of the solvent; W_{nM} is the Hamiltonian representing the nuclear degrees of freedom of the HFOA vibrations of the solute molecule.

Electromagnetic field (3) induces an optical polarization in the medium $\mathbf{P}(t)$ which can be expanded in powers of $\mathbf{E}(t)$ (Ref. 40)

$$\mathbf{P}^{(n)}(t) = N\mathrm{Tr}_R(\mathbf{D}\rho^{(n)}(t)), \tag{4}$$

where N is the density of particles in the system; $\mathbf{D}$ is the dipole moment operator of a solute molecule; $\rho^{(n)}$ is the density matrix of the system calculated in nth approximation with respect to $\mathbf{E}(t)$. The density matrix satisfies the Liouville equation:

$$i\hbar\frac{\partial\rho}{\partial t} = [H_0 + H'(t), \rho], \tag{5}$$

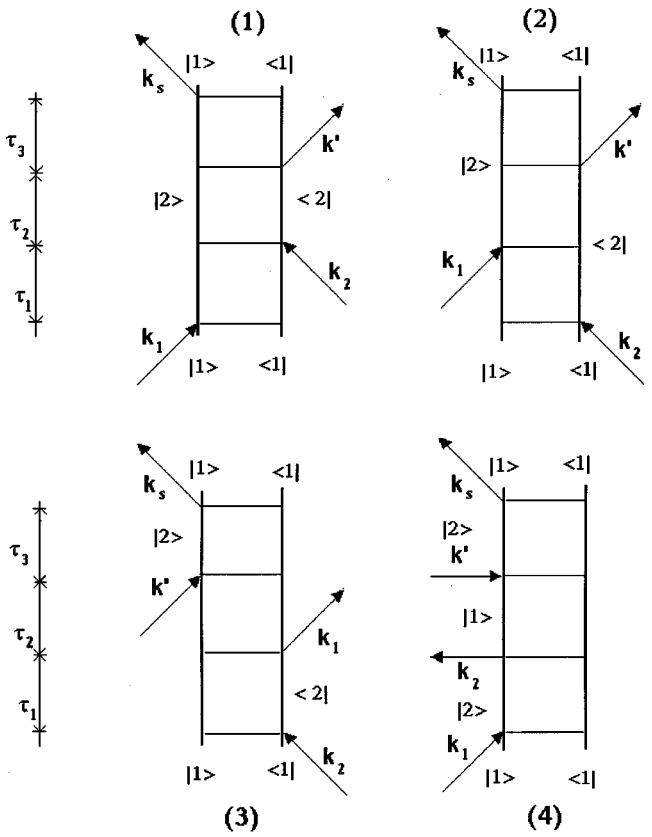

FIG. 1. Double sided Feynman diagrams for resonance four-photon interaction.

where $H'(t)=-\mathbf{DE}(t)$. The quantities $\rho^{(n)}$ can be conveniently displayed in the form of double-sided Feynman diagrams.[36,41]

Let us consider first double-sided Feynman diagrams for resonance four-photon interaction ($n=3$). The relevant diagrams are depicted in Fig. 1. It can be seen from the diagrams of Fig. 1 that odd times τ_1 and τ_3 determine the evolution of the nondiagonal elements of the density matrix corresponding to an optical electronic transition. The contribution from the low part of diagram (1) corresponding to the evolution during the time τ_1, is equal to

$$\frac{1}{\hbar^2}\int_0^\infty d\tau_1 \exp[-i(W_2/\hbar+\omega_{21}^{\mathrm{el}})\tau_1]\frac{1}{2}DE(t-\tau_1-\tau_2-\tau_3)$$
$$\times\exp[-i(t-\tau_1-\tau_2-\tau_3)\omega]\rho_{11}(-\infty)\exp\left(\frac{i}{\hbar}W_1\tau_1\right)$$
$$\times\tfrac{1}{2}DE^*(t-\tau_2-\tau_3)\exp[i(t-\tau_2-\tau_3)\omega], \tag{6}$$

where $\omega_{21}^{\mathrm{el}}=(E_2-E_1)/\hbar$ is the frequency of purely electronic transition $1\rightarrow 2$. This contribution amounts to a contribution from diagram (1) to a diagonal density matrix $\rho_{22}'^{(2)}(t-\tau_2-\tau_3)$.

A. Introducing rectangular vertices

Let us consider first the contribution to Eq. (6) from the LFOA vibrations $\{\omega_s\}$. In the case of appreciable Stokes losses when the perturbation of the nuclear system under electronic excitation $1\rightarrow 2$ (a quantity $V_s=W_{2s}-W_{1s}$) is large, one can use a semiclassical (short time) approximation.[42] As noted above, odd times τ_1, τ_3 and so on determine the evolution of the nondiagonal elements of the density matrix corresponding to an optical electronic transition. When electronic dephasing is fast, these times are very short and the short time or semiclassical approximation is applicable. Then the term $\exp[-i(W_{2s}/\hbar+\omega_{21}^{\mathrm{el}}-\omega)\tau_1]\times\rho_{11}(-\infty)\exp[(i/\hbar)W_{1s}\tau_1]$ in Eq. (6) can be represented in the following form:

$$\exp[-i(W_{2s}/\hbar+\omega_{21}^{\mathrm{el}}-\omega)\tau_1]\rho_{11}(-\infty)\exp\left(\frac{i}{\hbar}W_{1s}\tau_1\right)$$
$$\approx\exp[-i(V_s/\hbar+\omega_{21}^{\mathrm{el}}-\omega)\tau_1]\rho_{11}(-\infty). \tag{7}$$

In addition, the field amplitudes $\mathcal{E}(t)$ [see Eq. (1)] will not depend on odd times τ_1 and τ_3 for pump pulses long compared with electronic dephasing. As to the phase function $\varphi(t)$, we take into account only the linear changes of the field phase during odd times τ_{2j+1} which are of the order of the irreversible dephasing time T' (Ref. 24)

$$\varphi(t-\tau_1-\tau_2-\tau_3)\approx\varphi(t-\tau_2)-\frac{d\varphi(t-\tau_2)}{d(t-\tau_2)}(\tau_1+\tau_3). \tag{8}$$

Using Eqs. (6)–(8), we obtain for the contribution from the low part of diagram (1)

$$\rho_{22}'^{(2)}(t-\tau_2)$$
$$=\frac{1}{4\hbar^2}|D\mathcal{E}(t-\tau_2)|^2\int_0^\infty d\tau_1$$
$$\times\exp[-i(V_s/\hbar+\omega_{21}^{\mathrm{el}}-\omega(t-\tau_2))\tau_1]\rho_{11}(-\infty)$$
$$=\frac{1}{4\hbar^2}|D\mathcal{E}(t-\tau_2)|^2\left[i\frac{P}{\omega(t-\tau_2)-\omega_{21}^{\mathrm{el}}-V_s/\hbar}\right.$$
$$\left.+\pi\delta(\omega(t-\tau_2)-\omega_{21}^{\mathrm{el}}-V_s/\hbar)\right]\rho_{11}(-\infty), \tag{9}$$

where $\omega(t)=\omega-d\varphi(t)/dt$, P is the symbol for the principal value. In a similar manner, the contribution from the low part of diagram (2) can be presented in the form: $\rho_{22}''^{(2)}(t-\tau_2)=[\rho_{22}'^{(2)}(t-\tau_2)]^*$. We can sum the subdiagrams for $\rho_{22}'^{(2)}(t-\tau_2)$ and $\rho_{22}''^{(2)}(t-\tau_2)$. Using Eq. (9), we obtain

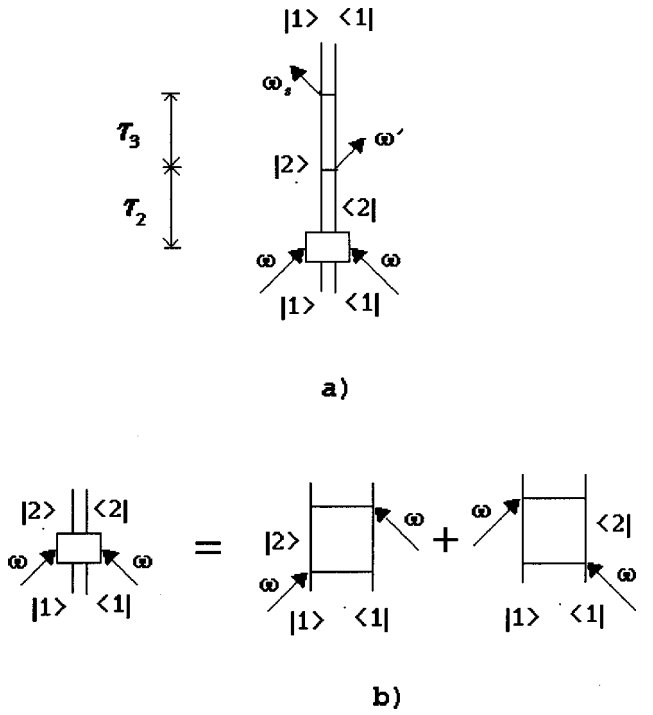

FIG. 2. Sum of double sided Feynman diagrams (1) and (2). The rectangular vertex represents the particle creation in the excited electronic state due to photon absorption.

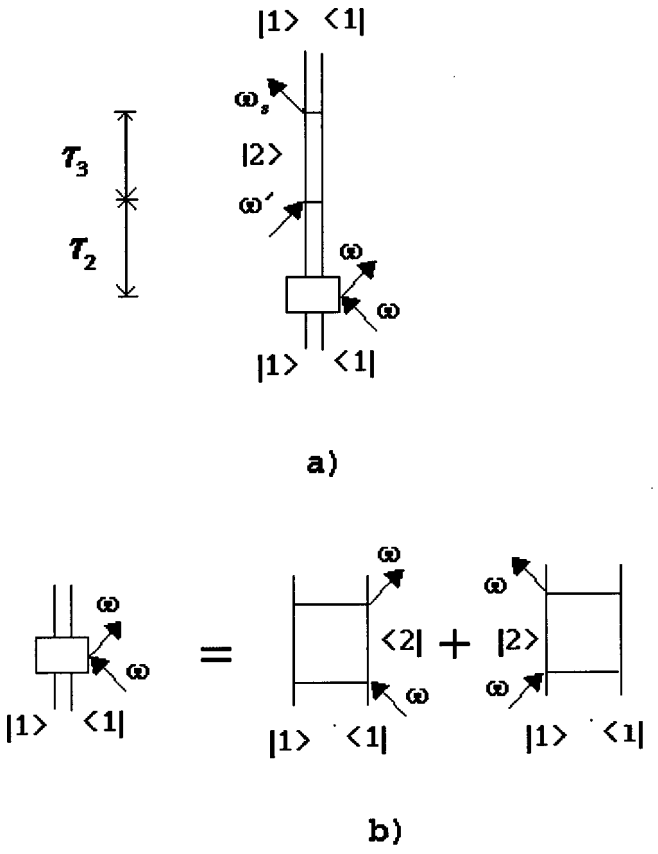

FIG. 3. Sum of double sided Feynman diagrams (3) and (4). The rectangular vertex represents the hole creation in the ground electronic state due to photon absorption.

$$\rho_{22}^{\prime(2)}(t-\tau_2)+\rho_{22}^{\prime\prime(2)}(t-\tau_2)$$
$$=\frac{1}{4\hbar^2}|D\mathcal{E}(t-\tau_2)|^2$$
$$\times\int_{-\infty}^{\infty}d\tau_1\exp[i(V_s/\hbar+\omega_{21}^{\mathrm{el}}-\omega(t-\tau_2))\tau_1]\rho_{11}(-\infty)$$
$$=\frac{\pi}{2\hbar^2}|D\mathcal{E}(t-\tau_2)|^2\delta(\omega(t-\tau_2)-\omega_{21}^{\mathrm{el}}-V_s/\hbar)\rho_{11}(-\infty). \tag{10}$$

Thus, one can combine the diagrams which differ in double lines $|2\rangle\langle 1|$ and $|1\rangle\langle 2|$ only.

The diagrams in pairs (1) and (2) and (3) and (4) differ in low double lines $|2\rangle\langle 1|$ and $|1\rangle\langle 2|$. Therefore, diagrams (1) and (2) can be combined into a single diagram shown in Fig. 2(a). The subdiagram with the rectangular vertex in this figure is equal to the sum of two subdiagrams shown in Fig. 2(b). In a similar manner, diagrams (3) and (4) can be combined into a single diagram displayed in Fig. 3(a) where the subdiagram with the rectangular vertex represents the sum of two subdiagrams shown in Fig. 3(b). It makes no difference whether the arrows are to the right or to the left of the subdiagram with the double horizontal line of Fig. 3.

We can generalize this consideration to the case of the calculation of the density matrix in any order with respect to applied field. Introducing rectangular vertices enables us to consider the density matrix diagonal with respect to electronic indices only. There exist three types of such vertices shown in Fig. 4. The contributions from the jth vertices of the a) and b) type in Fig. 4 are equal to

$$\text{a)}=\text{b)}=\frac{\pi}{2\hbar^2}|D\mathcal{E}(t-\tau_{2m}-\tau_{2m-2}-\cdots-\tau_{2j})|^2$$
$$\times\delta(\omega(t-\tau_{2m}-\tau_{2m-2}-\cdots-\tau_{2j})-\omega_{21}^{\mathrm{el}}-V_s/\hbar). \tag{11}$$

The contribution from the jth vertex of the c) type is of opposite sign: $\text{c)}=-a$.

The rectangular vertices correspond to the contact approximation[19,24,33,43] (an electronic optical transition occurs at the intersection of a photonic replication and the corresponding term).

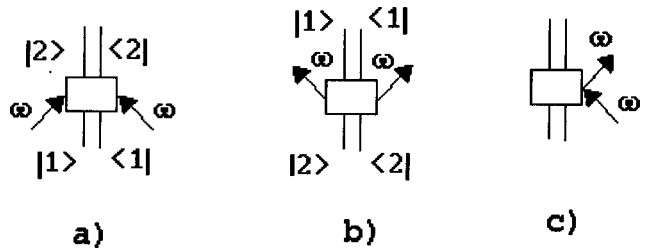

FIG. 4. Three types of rectangular vertices with double horizontal lines. Vertices a) and b) represent the particle creation in the excited electronic state (a) and in the ground electronic state (b) due to photon absorption and emission, respectively. Vertex c) represents the hole creation in the ground or excited electronic state due to photon absorption or emission, respectively.

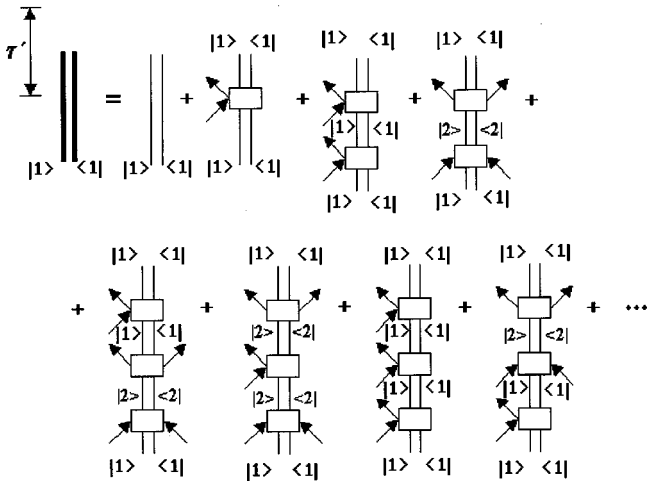

FIG. 5. Graphic representation of Eq. (12) for $n=1$. The first row of diagrams represents zero, second and fourth-order terms in the perturbation expansion. The second row represents sixth order terms. The second and higher order terms represent different sequential processes of the particle and hole creation and their evolution during ''even times'' (including τ') in the ground and excited electronic states.

The density matrix diagonal with respect to electronic indices can be represented as the sum of the even approximations with respect to the amplitude of an external field

$$\rho_{nn}(t)=\sum_{j=0}^{\infty}\rho_{nn}^{(2j)}(t), \tag{12}$$

where $\rho_{nn}^{(0)}(t)=\rho_{nn}(-\infty)$. Equation (12) is displayed graphically for $n=1$ in Fig. 5. Two thick vertical lines correspond to the complete density matrix. The number of the diagrams that contribute to $\rho_{nn}^{(2j)}(t)$ is equal to 2^{j-1}—the number of the Liouville space pathways by which one can achieve state $|n\rangle\langle n|$ beginning from $|1\rangle\langle 1|$.

B. Incorporating of optically active intramolecular vibrational modes

Now let us consider OA intramolecular vibrational modes. Then Eq. (10) can be rewritten in the form

$$\rho_{22}'^{(2)}(t-\tau_2)+\rho_{22}''^{(2)}(t-\tau_2)$$
$$=\frac{1}{4\hbar^2}|D\mathcal{E}(t-\tau_2)|^2\int_{-\infty}^{\infty}d\tau_1$$
$$\times\exp[i(V_s/\hbar+\omega_{21}^{\mathrm{el}}-\omega(t-\tau_2))\tau_1]$$
$$\times\exp\left(\frac{i}{\hbar}W_{2M}\tau_1\right)\rho_{11}(-\infty)\exp\left(-\frac{i}{\hbar}W_{1M}\tau_1\right). \tag{13}$$

Numerous experiments[44–50] show that the Franck–Condon molecular state achieved by an optical excitation, relaxes very fast and the relaxed intramolecular spectrum forms within 0.1 ps. Therefore, we shall consider that the intramolecular relaxation related to the OAHF vibrations takes place in a time shorter than the pump pulse duration. Such a picture corresponds to a rather universal dynamical behavior of large polar chromophores in polar solvents, which may be represented by four well-separated time scales:[50] An intramolecular vibrational component, and intermolecular relaxation which consists of an ultrafast (~100 fs), 1–4 ps, and 10–100 ps decay components. Of course, some of the LF intramolecular vibrations can relax with the rate of intermolecular relaxation. We include such vibrations into the system $\{\omega_s\}$.

Thus, we can consider the density matrix averaged with respect to the intramolecular OAHF vibrations

$$\rho_{ns}(t)=\mathrm{Tr}_M\rho_{nn}(t), \tag{14}$$

where the total density matrix $\rho_{nn}(t)$ is factorized

$$\rho_{nn}(t)=\rho_{nM}\rho_{ns}(t) \tag{15}$$

and

$$\rho_{nM}=\exp(-\beta W_{nM})/\mathrm{Tr}_M\exp(-\beta W_{nM}),$$

is the equilibrium density matrix of the intramolecular OAHF vibrations. Here Tr_M denotes the operation of taking a trace over the variables of the intramolecular OAHF vibrations, $\beta=1/(k_BT)$.

Calculating a trace Tr_M of both sides of Eq. (13), we obtain

$$\rho_{2s}'^{(2)}(t-\tau_2)+\rho_{2s}''^{(2)}(t-\tau_2)$$
$$=\frac{\pi}{2\hbar^2}|D\mathcal{E}(t-\tau_2)|^2$$
$$\times F_{1M}(\omega(t-\tau_2)-\omega_{21}^{\mathrm{el}}-V_s/\hbar)\rho_{1s}(-\infty),$$

where

$$F_{1,2M}(\omega')=\frac{1}{2\pi}\int_{-\infty}^{\infty}d\tau_1 f_{\alpha,\varphi M}(\tau_1)\exp(-i\omega'\tau_1), \tag{16}$$

are the ''intramolecular'' (M) absorption (1) or luminescence (2) spectra of a solute molecule

$$f_{\alpha,\varphi M}(\tau_1)=\mathrm{Tr}_M[\exp(\pm(i/\hbar)W_{2,1M}\tau_1)$$
$$\times\exp(\mp(i/\hbar)W_{1,2M}\tau_1)\rho_{1,2M}], \tag{17}$$

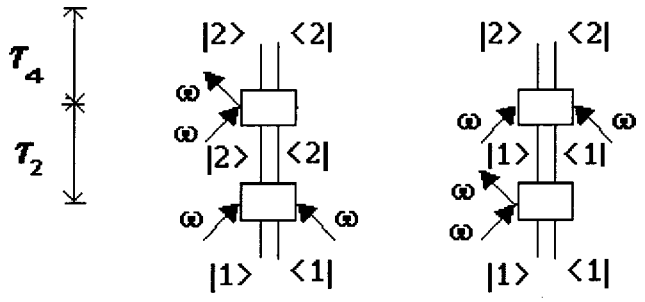

FIG. 6. The fourth-order contribution to $\rho_{2s}(t)$. The left diagram represents the particle creation in the excited electronic state due to photon absorption, the subsequent particle evolution in state 2 during time τ_2, then the hole creation in this state due to photon emission, and the subsequent hole evolution in the excited electronic state during time τ_4. The right diagram represents the hole creation in the ground electronic state due to photon absorption, the subsequent hole evolution in state 1 during time τ_2, then the particle creation in the excited electronic state due to photon absorption, and the subsequent particle evolution in state 2 during time τ_4.

are the characteristic functions (the Fourier transforms) of the intramolecular absorption (α) or emission (φ) spectrum.[42]

Generalizing this consideration, we arrive at the following results for the contributions from the jth vertices of the a), b), and c) type in Fig. 4:

$$\text{a)}=\frac{\pi}{2\hbar^2}|D\mathcal{E}(t-\tau_{2m}-\tau_{2m-2}-\cdots-\tau_{2j})|^2 \times F_{1M}(\omega(t-\tau_{2m}-\tau_{2m-2}-\cdots-\tau_{2j})-\omega_{21}^{\mathrm{el}}-V_s/\hbar), \tag{18}$$

$$\text{b)}=\frac{\pi}{2\hbar^2}|D\mathcal{E}(t-\tau_{2m}-\tau_{2m-2}-\cdots-\tau_{2j})|^2 \times F_{2M}(\omega(t-\tau_{2m}-\tau_{2m-2}-\cdots-\tau_{2j})-\omega_{21}^{\mathrm{el}}-V_s/\hbar), \tag{19}$$

$$\text{c)}=-\frac{\pi}{2\hbar^2}|D\mathcal{E}(t-\tau_{2m}-\tau_{2m-2}-\cdots-\tau_{2j})|^2 \times F_{nM}(\omega(t-\tau_{2m}-\tau_{2m-2}-\cdots-\tau_{2j})-\omega_{21}^{\mathrm{el}}-V_s/\hbar). \tag{20}$$

Comparing Eq. (11) with Eqs. (18)–(20), one can see that the first equation can be obtained from the last ones by replacing the intramolecular spectra F_{nM} with δ-functions. In contrast to the case of absence of OAHF modes, the contributions from the vertices of the a) and b) type distinct from each other when these modes are present.

C. Inclusion of damping

Consider the fourth order contribution with respect to the pump field to the density matrix $\rho_{2s}(t)$ in the Condon approximation. This contribution is described by two diagrams shown in Fig. 6

$$\rho_{2s}(t)=\rho_{2s}^{(2\leftarrow 1\leftarrow 1)}(t)+\rho_{2s}^{(2\leftarrow 2\leftarrow 1)}(t). \tag{21}$$

Each term on the right-hand-side of Eq. (21) can be written as the double convolution of the field factors and the ''evolutional'' part of the density matrix $\rho_{2s}^{ev(2\leftarrow n\leftarrow 1)}(\tau_4,\tau_2,t)$ ($n=1,2$) that is determined by the evolution in different electronic states

$$\rho_{2s}^{(2\leftarrow n\leftarrow 1)}(t)=-\int_0^\infty d\tau_4\int_0^\infty d\tau_2\frac{\pi}{2\hbar^2}|D\mathcal{E}(t-\tau_4)|^2 \times\frac{\pi}{2\hbar^2}|D\mathcal{E}(t-\tau_4-\tau_2)|^2\rho_{2s}^{ev(2\leftarrow n\leftarrow 1)}(\tau_4,\tau_2,t), \tag{22}$$

where

$$\rho_{2s}^{ev(2\leftarrow n\leftarrow 1)}(\tau_4,\tau_2,t) =\exp(-i\mathcal{L}_{2s}\tau_4)F_{nM}(\omega(t-\tau_4)-\omega_{21}^{\mathrm{el}}-V_s/\hbar) \times\exp(-i\mathcal{L}_{ns}\tau_2)F_{1M}(\omega(t-\tau_4-\tau_2)-\omega_{21}^{\mathrm{el}} -V_s/\hbar)\rho_{1s}(-\infty), \tag{23}$$

$\mathcal{L}_{ns}$ is the Liouville operator determined by the following expression: $\mathcal{L}_{ns}A=\hbar^{-1}[H_{ns},A]$, and $[\exp(-i\mathcal{L}_{ns}\tau)]_{klmp}=[\exp(-(i/\hbar)H_{ns}\tau)]_{km}[\exp(i/\hbar)H_{ns}\tau)]_{pl}$; $H_{ns}=E_n+W_{ns}$.

We next write Eq. (23) in the coordinate representation:

$$\langle\mathbf{Q}|\rho_{2s}^{ev(2\leftarrow n\leftarrow 1)}(\tau_4,\tau_2,t)|\mathbf{Q}'\rangle =\int d\mathbf{Q}''\int d\mathbf{Q}'''\int d\mathbf{Q}^{\mathrm{IV}}\int d\mathbf{Q}^{\mathrm{V}} \times\langle\mathbf{Q}|\exp(-iH_{2s}\tau_4/\hbar)|\mathbf{Q}''\rangle F_{nM}(\omega(t-\tau_4)-\omega_{21}^{\mathrm{el}} -V_s(\mathbf{Q}'')/\hbar)\langle\mathbf{Q}''|\exp(-iH_{ns}\tau_2/\hbar)|\mathbf{Q}'''\rangle \times F_{1M}(\omega(t-\tau_4-\tau_2)-\omega_{21}^{\mathrm{el}}-V_s(\mathbf{Q}''')/\hbar) \times\langle\mathbf{Q}'''|\rho_{1s}(-\infty)|\mathbf{Q}^{\mathrm{IV}}\rangle\langle\mathbf{Q}^{\mathrm{IV}}|\exp(iH_{ns}\tau_2/\hbar)|\mathbf{Q}^{\mathrm{V}}\rangle \times\langle\mathbf{Q}^{\mathrm{V}}|\exp(iH_{2s}\tau_4/\hbar)|\mathbf{Q}'\rangle, \tag{24}$$

and introduce new coordinates

$$\frac{\mathbf{Q}+\mathbf{Q}'}{2}=\mathbf{q},\quad \mathbf{Q}-\mathbf{Q}'=\mathbf{q}'. \tag{25}$$

Here $\mathbf{Q}$ is a vector coordinate of the LFOA vibrations $\{\omega_s\}$.

Let us consider the Wigner representation[41,51–53] of the evolutional part of the density matrix and the corresponding operators (A)

$$\rho_{2sW}^{ev(2\leftarrow n\leftarrow 1)}(\mathbf{q},\mathbf{p};\tau_4,\tau_2,t) =\frac{1}{(2\pi\hbar)^{N_d}}\int_{-\infty}^{\infty}\left\langle\mathbf{q}+\frac{\mathbf{q}'}{2}\middle|\rho_{2s}^{ev(2\leftarrow n\leftarrow 1)}(\tau_4,\tau_2,t)\middle|\mathbf{q}-\frac{\mathbf{q}'}{2}\right\rangle \times\exp\left(-\frac{i}{\hbar}\mathbf{p}\mathbf{q}'\right)d\mathbf{q}', \tag{26}$$

$$A_W(\mathbf{q},\mathbf{p};t)=\int_{-\infty}^{\infty}\left\langle\mathbf{q}+\frac{\mathbf{q}'}{2}\middle|A(t)\middle|\mathbf{q}-\frac{\mathbf{q}'}{2}\right\rangle \times\exp\left(-\frac{i}{\hbar}\mathbf{p}\mathbf{q}'\right)d\mathbf{q}',$$

where N_d is the number of the degrees of freedom of the system $\{\omega_s\}$.

We next consider the classical (high-temperature) approximation. In the high-temperature approximation the density matrix of the ground-state $\rho_{1s}(-\infty)$ can be written in the form (see Ref. 54)

$$\langle\mathbf{Q}|\rho_{1s}(-\infty)|\mathbf{Q}'\rangle=\exp\left[-\frac{(\mathbf{Q}-\mathbf{Q}')^2}{2\hbar^2\beta}-\beta U_{1s}\left(\frac{\mathbf{Q}+\mathbf{Q}'}{2}\right)\right] \times\left(\int_{-\infty}^{\infty}\exp[-\beta U_{1s}(\mathbf{Q})]d\mathbf{Q}\right)^{-1}, \tag{27}$$

where U_{1s} is the potential energy of the system $\{\omega_s\}$ in the electronic state 1.

The Wigner representation of $\langle \mathbf{Q}|\rho_{1s}(-\infty)|\mathbf{Q}'\rangle$ is the classical density matrix

$$\rho_{1sW}(\mathbf{q},\mathbf{p};-\infty)=\left(\frac{\beta}{2\pi}\right)^{N_d/2}\exp\left[-\frac{\beta\mathbf{p}^2}{2}-\beta U_{1s}(\mathbf{q})\right]\times\left(\int_{-\infty}^{\infty}\exp[-\beta U_{1s}(\mathbf{q})]d\mathbf{q}\right)^{-1}. \quad (28)$$

It is well-known that an operator depending on the coordinates alone [like $F_{nM}(\omega(t-\tau_4)-\omega_{21}^{\mathrm{el}}-V_s(\mathbf{Q}'')/\hbar)$] will retain its form in the Wigner representation. Therefore, we drop the subscript W near the corresponding operators. In the classical case the Wigner representation of $\langle \mathbf{Q}|\exp(-iH_{2s}\tau_4)|\mathbf{Q}''\rangle\langle \mathbf{Q}^{\mathrm{V}}|\exp(iH_{2s}\tau_4)|\mathbf{Q}'\rangle$ is the Liouville space Green function $\mathcal{G}_{2c}(\mathbf{pq}\tau_4;\mathbf{p}'\mathbf{q}')$ that obeys the classical Liouville equation. Thus, we obtain for $\rho_{2sW}^{ev(2\leftarrow n\leftarrow 1)}(\mathbf{q},\mathbf{p};\tau_4,\tau_2,t)$:

$$\rho_{2sW}^{ev(2\leftarrow n\leftarrow 1)}(\mathbf{q},\mathbf{p};\tau_4,\tau_2,t)=\int d\mathbf{q}'\int d\mathbf{p}'\int d\mathbf{q}''\int d\mathbf{p}''\mathcal{G}_{2c}(\mathbf{pq}\tau_4;\mathbf{p}'\mathbf{q}')F_{nM}(\omega(t-\tau_4)-\omega_{21}^{\mathrm{el}}-V_s(\mathbf{q}')/\hbar)\mathcal{G}_{nc}(\mathbf{p}'\mathbf{q}'\tau_2;\mathbf{p}''\mathbf{q}'')\times F_{1M}(\omega(t-\tau_4-\tau_2)-\omega_{21}^{\mathrm{el}}-V_s(\mathbf{q}'')/\hbar)\left(\frac{\beta}{2\pi}\right)^{N_d/2}\exp\left[-\frac{\beta\mathbf{p}''^2}{2}-\beta U_{1s}(\mathbf{q}'')\right]\left(\int_{-\infty}^{\infty}\exp[-\beta U_{1s}(\mathbf{q})]d\mathbf{q}\right)^{-1}. \quad (29)$$

The Liouville space Green function $\mathcal{G}_{2c}(\mathbf{pq}\tau_4;\mathbf{p}'\mathbf{q}')$ in Eq. (29) represents the nuclear propagation from the phase space $\{\mathbf{p}'\mathbf{q}'\}$ to $\{\mathbf{pq}\}$ in the electronic state 2. It is conveniently to use a reduced description, when $\{\mathbf{pq}\}$ represents only a partial set of coordinates related to optically active modes $\{\omega_s\}$ which give a contribution to $V_s(\mathbf{q})$. The effect of the remaining modes can be introduced through a random force and friction in the Langevin equation.[55] Using standard techniques, one can then obtain a Fokker–Planck equation for the Green function in the reduced space.[41,53,56–58] Classical low-frequency intramolecular and solvent modes are usually overdamped. Since, in this case the momentum rapidly approaches its equilibrium value, it needs not be considered an independent variable. The Liouville space Green function then satisfies a Fokker–Planck equation in the configuration coordinate space, and we obtain for one-dimensional reduced space

$$\left(\frac{\partial}{\partial t}-L_{ns}\right)\mathcal{G}_{nc}(q,t;q')=0,\quad \mathcal{G}_{nc}(q,0;q')=\delta(q-q'), \quad (30)$$

where L_{ns} is the Fokker–Planck operator in the electronic state n. It can be written in the form: $L_{ns}=\tilde{D}_n(\partial/\partial q)\times((\partial/\partial q)+\beta(\partial/\partial q)U_{ns}(q))$ where $\tilde{D}_n$ and $U_{ns}(q)$ are the diffusion coefficient and the potential energy, respectively, in electronic state n.

In the case under consideration Eq. (29) may be transformed into the following equation:

$$\rho_{2s}^{ev(2\leftarrow n\leftarrow 1)}(q,\tau_4,\tau_2,t)=\int_{-\infty}^{\infty}dq'\int_{-\infty}^{\infty}dq''\mathcal{G}_{2c}(q,\tau_4;q')F_{nM}(\omega(t-\tau_4)-\omega_{21}^{\mathrm{el}}-V_s(q')/\hbar)\mathcal{G}_{nc}(q',\tau_2;q'')\times F_{1M}(\omega(t-\tau_4-\tau_2)-\omega_{21}^{\mathrm{el}}-V_s(q'')/\hbar)\rho_{1s}(q'',-\infty), \quad (31)$$

where

$$\rho_{1s}(q'',-\infty)=\left(\frac{\beta}{2\pi}\right)^{1/2}\exp[-\beta U_{1s}(q'')]\times\left(\int_{-\infty}^{\infty}\exp[-\beta U_{1s}(q)]dq\right)^{-1}. \quad (32)$$

Equations (22) and (31) enable us to write directly an expression for the corresponding diagram of Fig. 6. Such a procedure can be easily generalized to the calculation of any diagram.

When OAHF intramolecular vibrations are absent, the intramolecular spectra F_{nM} in Eq. (31) convert to δ-functions. Then integrating Eq. (31) with respect to q' and q'', we obtain

$$\rho_{22}^{ev(2\leftarrow n\leftarrow 1)}(q,\tau_4,\tau_2,t)=\hbar^2\sum_{i,j}|V'[q_j(t-\tau_4)]|^{-1}|V'[q_i(t-\tau_4-\tau_2)]|^{-1}\times\mathcal{G}_{2c}(q,\tau_4;q_j(t-\tau_4))\mathcal{G}_{nc}(q_j(t-\tau_4),\tau_2;q_i(t-\tau_4-\tau_2))\rho_{11}(q_i(t-\tau_4-\tau_2),-\infty), \quad (33)$$

where $V'(q_i)\equiv(dV/dq)|_{q=q_i}$ and $q_{i,j}(t-\tau')$ are the solutions of the equation

$$\omega(t-\tau')-\omega_{21}^{\mathrm{el}}-V(q)/\hbar=0. \quad (34)$$

The quantities $q_i(t-\tau')$ are the intersections of the moving photonic replications with the corresponding terms.[24]

D. Double-sided Feynman diagrams for fast optical dephasing

Let us consider the density matrix averaged with respect to the intramolecular OAHF vibrations $\rho_{ns}(t)$. It is represented by two vertical lines. The left line represents the

ket-$|n\rangle$ and the right line represents the bra-vector $\langle n|$. We can state the following rules for the double-sided Feynman diagrams for fast optical dephasing and a Markovian random evolution in the configuration coordinate space:

(1) The system evolution depends only on ''even'' times. Time increases from bottom to top;

(2) the interactions between system and the pump fields of frequency ω are presented by three types of the rectangular vertices (see Fig. 4). The vertex of the a) type corresponds to electronic transition $1\rightarrow 2$, the vertex of the b) type—to electronic transition $2\rightarrow 1$, and the vertex of the c) type does not change an electronic state;

(3) interactions with applied pump fields are labeled by the pairs of arrows. The contributions from the jth vertices of the a)–c) types in Fig. 4 are determined by Eqs. (18)–(20), respectively, where $V_s \equiv V_s(q)$. In the absence of intramolecular OAHF vibrations the corresponding contributions are equal to

$$\text{a)}=\text{b)}=-\text{c)} = \frac{\pi}{2\hbar^2}|D\mathcal{E}(t-\tau_{2m}-\tau_{2m-2}-\cdots-\tau_{2j})|^2\hbar \times \sum_i |V'[q_i(t-\tau_{2m}-\tau_{2m-2}-\cdots-\tau_{2j})]|^{-1}, \quad (35)$$

where $q_i(t-\tau')$ are the solutions of Eq. (34);

(4) the system evolution between adjacent rectangular vertices j and $j+1$ along the double vertical line in electronic state n is described by the corresponding Liouville space Green function $\mathcal{G}_{nc}(q_{j+1},\tau_{2j};q_j)$. The evolution of the system in a last even time τ_{2m} is described by the term $\mathcal{G}_{nc}(q,\tau_{2m};q_m)$.

In the absence of intramolecular OAHF vibrations, the system evolution between adjacent rectangular vertices j and $j+1$ along the double vertical line in electronic state n is described by $\mathcal{G}_{nc}(q_{i'}(t-\tau_{2m}-\cdots-\tau_{2j+2}),\tau_{2j};q_i(t-\tau_{2m}-\cdots-\tau_{2j}))$. The evolution of the system in a last even time τ_{2m} is described by the term $\mathcal{G}_{nc}(q,\tau_{2m};q_i(t-\tau_{2m}))$;

(5) the contribution from each diagram to $\rho_{ns}^{(2m)}(t)$ is obtained by integration with respect to all times $\tau_2,\tau_4,\ldots,\tau_{2m}$ and all coordinates $q_1,q_2,\ldots,q_m$. The space integration is eliminated in the absence of the intramolecular OAHF vibrations.

E. Summation of diagrams

Let us consider the density matrix $\rho_{nn}(t)$ [see Eq. (12)]. The same equation can be written also for $\rho_{ns}(t)$ that is displayed graphically for $n=1$ in Fig. 5.

If we detach from each term of the series of Fig. 5, from the second onwards, one rectangle and the line to its upper side, the remaining series, excluding terms resulting in the density matrix of the excited state, is again the complete density matrix $\rho_{1s}(t)$. Thus, the latter can be represented graphically by the diagrams displayed in Fig. 7(a). Analytically, this is written

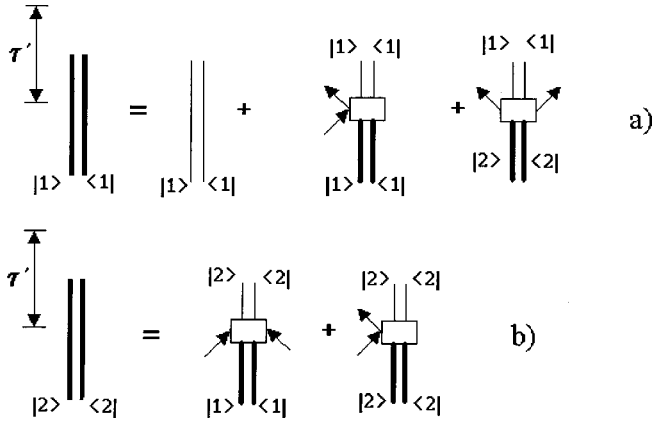

FIG. 7. Graphic summation of diagrams for $\rho_{1s}(t)$ (a) and $\rho_{2s}(t)$ (b). a: the first diagram on the right-hand-side represents the unperturbated density matrix; the second one is equal to the sum of all the diagrams resulting to the ground electronic state through the hole creation in state 1 (in particular, the second, third, fifth and seventh diagrams on the right-hand-side of the diagram equation shown in Fig. 5 contribute to this diagram); the third diagram on the right-hand-side represents the sum of all the diagrams resulting to the ground electronic state through the particle creation due to photon emission (the fourth, sixth and eighth diagrams on the right-hand-side of the diagram equation shown in Fig. 5 contribute to this diagram). b: the first diagram on the right-hand-side is equal to the sum of all the diagrams resulting to the excited electronic state through the particle creation due to photon absorption; the second one represents the sum of all the diagrams resulting to the excited electronic state through the hole creation due to photon emission.

$$\rho_{ns}(q,t)=\rho_{ns}(q,-\infty)+(-1)^n\frac{\pi}{2\hbar^2}\int_0^\infty d\tau'|D\mathcal{E}(t-\tau')|^2 \times \int_{-\infty}^{\infty} dq'\mathcal{G}_{nc}(q,\tau';q')[F_{1M}(\omega(t-\tau')-\omega_{21}^{\mathrm{el}} - V_s(q')/\hbar)\rho_{11}(q',t-\tau')-F_{2M}(\omega(t-\tau')-\omega_{21}^{\mathrm{el}} - V_s(q')/\hbar)\rho_{22}(q',t-\tau')], \quad (36)$$

for $n=1$. In a similar manner, the complete density matrix $\rho_{2s}(t)$ can be represented graphically by the diagrams displayed in Fig. 7(b). Analytically, this is written by Eq. (36) for $n=2$.

If we will denote $x=t-\tau'$, then $\int_0^\infty d\tau' \rightarrow \int_{-\infty}^t dx$. Let us assume that $\mathcal{E}(x)\equiv 0$ for $-\infty<x\leqslant 0$. Then $\int_{-\infty}^t dx \rightarrow \int_0^t dx$, and we obtain

$$\rho_{ns}(q,t)=\rho_{ns}^{(0)}(q) + (-1)^n\frac{\pi}{2\hbar^2}\int_0^t dx|D\mathcal{E}(x)|^2\int_{-\infty}^{\infty} dq' \times \mathcal{G}_{nc}(q,t-x;q')[F_{1M}(\omega(x)-\omega_{21}^{\mathrm{el}}-V_s(q')/\hbar) \times \rho_{1s}(q',x)-F_{2M}(\omega(x)-\omega_{21}^{\mathrm{el}} - V_s(q')/\hbar)\rho_{2s}(q',x)], \quad (37)$$

where $\rho_{ns}^{(0)}(q)=\rho_{ns}(q,-\infty)$. Equation (37) is a central result of this work. It generalizes Eq. (15) of Ref. 24 to the case of the excitation of quantum intramolecular modes. In addition, Eq. (37) extends the last equation to anharmonic potentials $U_{ns}(q)$ which can be of different shape in electronic states 1

and 2. The quantities $F_{1,2M}(\omega(x)-\omega_{21}^{\mathrm{el}}-V_s(q')/\hbar)$, appearing in Eq. (37), are the intramolecular absorption (1) and luminescence (2) spectra. They cannot be measured directly for a molecule which is in a polar solvent. However, the intramolecular spectra $F_{1,2M}$ can be determined as the spectra of the same solute in a nonpolar solvent.[59]

Integrating the both side of Eq. (37) with respect to q, we obtain

$$\langle\rho\rangle_{nn}(t)=\delta_{n1}+(-1)^n\frac{\pi}{2\hbar^2}\int_0^t dx|D\mathcal{E}(x)|^2 \times\int_{-\infty}^{\infty}dq'[F_{1M}(\omega(x)-\omega_{21}^{\mathrm{el}}-V_s(q')/\hbar) \times\rho_{1s}(q',x)-F_{2M}(\omega(x)-\omega_{21}^{\mathrm{el}} -V_s(q')/\hbar)\rho_{2s}(q',x)], \tag{38}$$

where δ_{ij} is the Kronecker delta, $\langle\rho\rangle_{jj}(t)=\int\rho_{js}(q,t)dq$ is the normalized population of electronic state j, i.e., $\langle\rho\rangle_{jj}(t)\equiv n_j$, $n_1+n_2=1$. Equation (38) is the generalization of Eq. (20) of Ref. 24 to the case of the excitation of quantum intramolecular modes.

III. THE EFFECT OF HIGH-FREQUENCY INTRAMOLECULAR MODES ON CHIRPED PULSE EXCITATION

Let us assume that the potentials $U_{ns}(q)$ are harmonic: $U_{ns}(q)=E_n+\frac{1}{2}\tilde{\omega}^2(q-\delta_{n2}d)^2$. Then $V_s(q)=\hbar\omega_{st}/2-q\tilde{\omega}^2d$, where $\omega_{st}=\tilde{\omega}^2d^2/\hbar$ is the contribution of the OALF vibrations $\{\omega_s\}$ to the Stokes shift of the equilibrium absorption and luminescence spectra. As to quantum intramolecular modes, we will consider one normal intramolecular oscillator of frequency ω_0 whose equilibrium position is shifted under electronic transition. Its characteristic functions $f_{\alpha,\varphi M}(\tau_1)$ are determined by the following expression:[60]

$$f_{\alpha,\varphi M}(\tau_1)=\exp(-S_0\coth\theta_0) \times\sum_{k=-\infty}^{\infty}I_k(S_0/\sinh\theta_0)\exp[k(\theta_0\pm i\omega_0\tau_1)], \tag{39}$$

where S_0 is the dimensionless parameter of the shift, $\theta_0=\hbar\omega_0/(2k_BT)$, $I_n(x)$ is the modified Bessel function of first kind.[61] Substituting this expression into Eq. (16) and using Eq. (38), we get

$$n_2(t)=1-n_1(t) =\sqrt{2\pi\sigma_{2s}}\int_0^t dx\sum_{k=-\infty}^{\infty}w_k(x)[\tilde{\rho}_{11}(\omega_{21}+k\omega_0 -\omega(x),x)-\tilde{\rho}_{22}(\omega_{21}-k\omega_0-\omega(x),x)], \tag{40}$$

where

$$w_k(t)=\exp(-S_0\coth\theta_0)I_k \times(S_0/\sinh\theta_0)\exp(k\theta_0)\sigma_a(\omega_{21})J(t), \tag{41}$$

are the probabilities of light-induced transitions at $\alpha=\omega_{21}\pm k\omega_0-\omega(x)$, $\omega_{21}=\omega_{21}^{\mathrm{el}}+\omega_{st}/2$ is the frequency of Franck–Condon transition $1\rightarrow2$ with respect to the configuration coordinate related to $\{\omega_s\}$. Here we introduced a new variable $\alpha=qd\tilde{\omega}^2/\hbar$ so that $\rho_{nn}(q,t)dq=\tilde{\rho}_{nn}(\alpha,t)d\alpha$. The quantity $\sigma_a(\omega_{21})$ in Eq. (41) is the value of the cross section corresponding to the maximum of the absorption band in the absence of hf intramolecular modes,[24] $J(t)$ is the power density of the exciting radiation, $\sigma_{2s}=\omega_{st}/(\hbar\beta)$ is the contribution of the OALF vibrations $\{\omega_s\}$ to a second central moment of an absorption spectrum, so that $\sqrt{2\pi\sigma_{2s}}\sigma_a(\omega_{21})J(t)=\hbar^{-2}(\pi/2)|D\mathcal{E}(t)|^2$.

To obtain a differential equation for the quantity $\tilde{\rho}_{ns}(\alpha,t)$, we use Eqs. (16), (30), (37), (39), (41), and differentiate both sides of Eq. (37) with respect to t:

$$\frac{\partial}{\partial t}\tilde{\rho}_{ns}(\alpha,t)=\tilde{L}_{ns}\tilde{\rho}_{ns}(\alpha,t)+(-1)^n\sqrt{2\pi\sigma_{2s}}\sum_{k=-\infty}^{\infty}w_k(t) \times[\delta(\omega_{21}+k\omega_0-\omega(t)-\alpha)\tilde{\rho}_{1s}(\alpha,t) -\delta(\omega_{21}-k\omega_0-\omega(t)-\alpha)\tilde{\rho}_{2s}(\alpha,t)], \tag{42}$$

where

$$\tilde{L}_{ns}=\tau_{sn}^{-1}\left[1+(\alpha-\delta_{n2}\omega_{st})\frac{\partial}{\partial(\alpha-\delta_{n2}\omega_{st})} +\sigma_{2s}\frac{\partial^2}{\partial(\alpha-\delta_{n2}\omega_{st})^2}\right], \tag{43}$$

$\tau_{sn}=\sigma_{2s}/\tilde{D}_n$ is the correlation time in state n. Below we assume $\tau_{s1}=\tau_{s2}\equiv\tau_s$.

Equations (40) and (42) make it clear that the optical transitions occur not only at $\alpha=\omega_{21}-\omega(x)$, but at $\alpha=\omega_{21}\pm k\omega_0-\omega(x)$ also, where $k\neq0$. Therefore, $\tilde{\rho}_{ns}(\alpha,t)$ depends on $\tilde{\rho}_{1s}(\omega_{21}+k\omega_0-\omega(t),t)$ and $\tilde{\rho}_{2s}(\omega_{21}-k\omega_0-\omega(t),t)$ for different k resulting in the interference of different channels for optical transitions. It has been known[31] that the interference effects in the electron transfer reactions are of considerable significance for the inverted region. However, the role of these effects increases in importance for optical transitions under the action of chirped pulses. The point is that, first, one can realize all the Marcus regions in one experiment with chirped pulses: the normal region, the activationless region, and the inverted region. Second, the optical transitions in our model are controlled by diffusion to or from the intersection points (depending on the electronic state under consideration), because the holes (or spikes) in the distribution appear around the intersection points. The channels will be independent only if the holes (or spikes) do not overlap. However, the sliding of the intersection of photonic replication and the corresponding term along the term for chirped pulses[24] results in a delocalization of the holes (spikes) that increases the probability of their overlapping. Therefore, the interference arises between different channels of optical transitions which can not be considered separately.

We have solved Eq. (42) numerically assuming that for HF intramolecular modes $\hbar\omega_0\gg k_BT$. Then

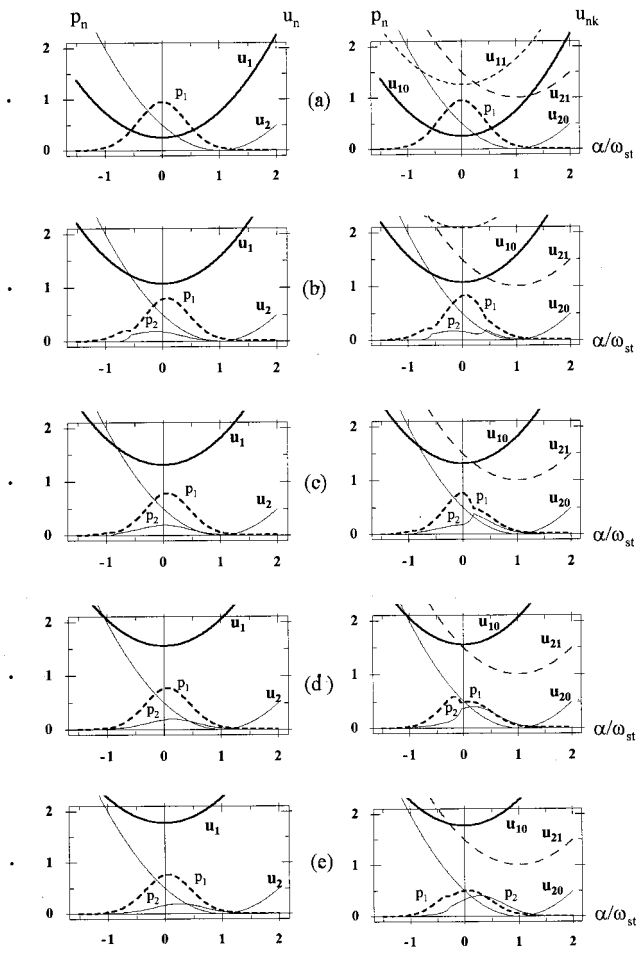

FIG. 8. Dimensionless nonequilibrium populations of molecular electronic states $p_n(\alpha,t)\equiv\omega_{st}\tilde{\rho}_{ns}(\alpha,t)$ with (right column) and without (left column) OAHF intramolecular modes at different time moments $(t-t_0)/t_p=-1.3$ (a), -0.27 (b), 0.03 (c), 0.33 (d), 0.6 (e). Other parameters are: $(\omega-\omega_{21})/\omega_{st}=0.8$, $\hbar\omega_{st}/(2k_BT)=2.834$, $Q'\equiv\sigma_a(\omega_{21})J_{\max}t_p=2.5$, $\tau_s/t_p=2$, $-\mu t_p/\omega_{st}=0.8$, $\omega_0/\omega_{st}=1$, $S_0=0.3$ (right column) and 0 (left column). $u_{2k}=\hbar(\alpha-\omega_{st})^2/(2\omega_{st}^2)+k\omega_0/\omega_{st}$ and $u_{1k}=\hbar\alpha^2/(2\omega_{st}^2)+k\omega_0/\omega_{st}+[\omega(t)-\omega_{21}^{el}]/\omega_{st}$ are dimensionless potentials corresponding to the excited state 2 (u_{2k}) and the photonic replication $1'$ of the ground state (u_{1k}), respectively. $k=0$ and 1 correspond to the vibrationless state and the first vibrationally excited state, respectively, with reference to the HF intramolecular mode ω_0. $u_n\equiv u_{n0}$.

$$w_k(t)=\exp(-S_0)\frac{S_0^k}{k!}\sigma_a(\omega_{21})J(t), \tag{44}$$

where $k\geqslant 0$. We used the following initial condition:

$$\tilde{\rho}_{nn}^{(0)}(\alpha)=\delta_{n1}(2\pi\sigma_{2s})^{-1/2}\exp[-\alpha^2/(2\sigma_{2s})]. \tag{45}$$

The normalized populations of electronic states can be calculated using Eq. (40), or by direct integration of $\tilde{\rho}_{ns}(\alpha,t)$ with respect to α

$$n_j(t)=\int\tilde{\rho}_{js}(\alpha,t)d\alpha. \tag{46}$$

We are interested in studying the effect of quantum intramolecular modes on the chirped pulse excitation in condensed phase. The calculation results, obtained by Eq. (46) and the numerical solution of Eq. (42) for a Gaussian pulse of the shape

$$E(t)\equiv\mathcal{E}(t)\exp(i\varphi(t))=\mathcal{E}_0\exp[-\tfrac{1}{2}(\delta^2-i\mu)(t-t_0)^2], \tag{47}$$

are shown in Figs. 8–10. The inset to Figs. 9 and 10(a) show equilibrium spectra of the absorption and the emission of

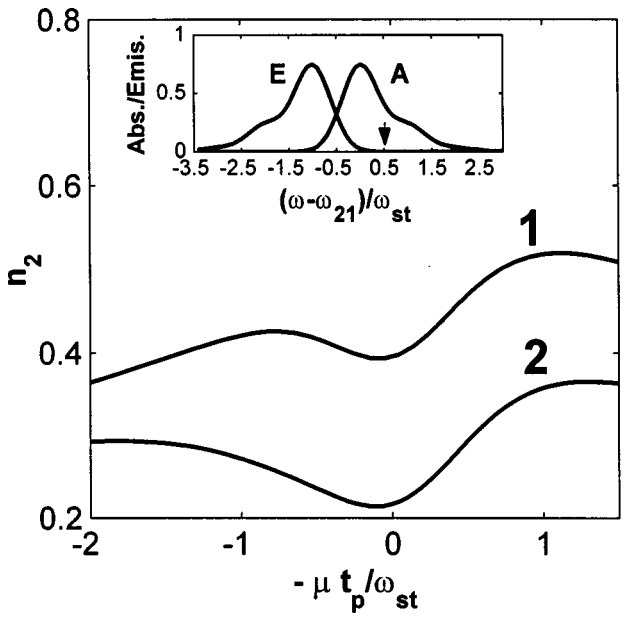

FIG. 9. The excited-state population n_2 after the completion of the pulse action as a function of the linear chirp rate μ with (1) and without (2) OAHF intramolecular modes. The parameters are: $(\omega-\omega_{21})/\omega_{st}=0.5$, $\hbar\omega_{st}/(2k_BT)=2.834$, $Q'\equiv\sigma_a(\omega_{21})J_{\max}t_p=2.5$, $\tau_s/t_p=2$, $\omega_0/\omega_{st}=1$, $S_0=0.3$ (1) and 0 (2). Inset: Equilibrium spectra of the absorption (A) and the emission (E); the arrow shows the relative position of the carrier frequency ω.

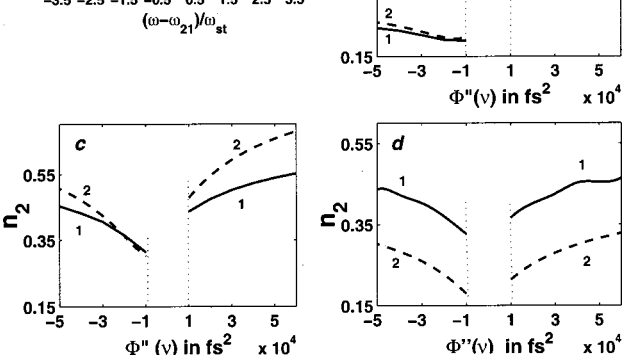

FIG. 10. The excited-state population n_2 after the completion of the pulse action as a function of the phase term $\Phi''(\nu)$ with (1) and without (2) OAHF intramolecular modes (b–d). The detunings $(\omega-\omega_{21})/\omega_{st}$ are equal to -0.5 (b), 0 (c) and 0.8 (d); other parameters are: $\hbar\omega_{st}/(2k_BT)=3.38$, $Q'\equiv\sigma_a(\omega_{21})J_{\max}t_p=2.5$, $\tau_s=70$ fs, $\tau_{p0}=11$ fs, $\omega_0/\omega_{st}=1$, $S_0=0.3$ (1) and 0 (2). a: Equilibrium spectra of the absorption (A) and the emission (E); the arrows b, c and d show the relative positions of the carrier pulse frequency ω for Figs. b–d, respectively.

model systems. One can see a progression with respect to an OAHF vibration. Each member of this progression is broadened mainly due to the presence of LFOA vibrations $\{\omega_s\}$, because the OAHF mode is underdamped [see Eq. (39)].

Figure 8 depicts the nonequilibrium populations of molecular electronic states 1 and 2 at different time moments when a molecule is excited using a positively chirped pulse ($\mu<0$). For comparison the left column shows the corresponding dependences $\tilde{\rho}_{ns}(\alpha,t)$ in the absence of the OAHF intramolecular modes. One can see peculiarities in the quantities $\tilde{\rho}_{ns}(\alpha,t)$ [spikes in $\tilde{\rho}_{2s}(\alpha,t)$ and holes in $\tilde{\rho}_{1s}(\alpha,t)$] corresponding to the instantaneous intersections between a moving photonic replication and the corresponding term, involving distinct intramolecular vibrational excitations. It is seen that the presence of high-frequency quantum modes (the right column) gives rise to parallel vibronic channels, which directly influence on the excitation of a molecule.

Let us study the influence of the chirp rate on the integral excited state population n_2 after the completion of pulse action. Experimentally, one measures the integrated fluorescence which is directly proportional to n_2. Figure 9 shows the effect of HF intramolecular modes on the excited state population n_2 as a function of the linear chirp rate $\mu(d\varphi/dt=\mu t)$. Experimentally, the chirped pulses are obtained by changing the separation of pulse compression gratings. Then the parameters δ and μ are determined by the formulas[13,24]

$$\delta^2=2\{\tau_{p0}^2+[2\Phi''(\omega)/\tau_{p0}]^2\}^{-1},$$
$$\mu=-4\Phi''(\omega)[\tau_{p0}^4+4\Phi''^2(\omega)]^{-1}, \tag{48}$$

where $\Phi''(\omega)=\Phi''(\nu)/(4\pi^2)$ is the phase term. Therefore, Fig. 10 shows n_2 as a function of the phase term. One can see from Figs. 9 and 10 that incorporating the intramolecular modes increases n_2 due to the parallel vibronic channels (see Fig. 8) when a molecule is excited near the $0\rightarrow1$ transition with respect to the OAHF vibration [Figs. 9 and 10(d)]. If the molecule is excited near the $0\rightarrow0$ transition with respect to the OAHF intramolecular mode, the effect is opposite [Figs. 10(b) and 10(c)].

These results can be explained by the picture of two-dimensional potentials corresponding to the OA underdamped HF mode and LF vibrations (see Fig. 11). If the pulse frequency corresponds to the $0\rightarrow1$ transition, the first field interaction excites a molecule to the first excited level of the intramolecular HF vibration. This intramolecular excitation relaxes very fast to the vibrationless state of this vibration (the HF mode is in equilibrium in the time scale under consideration). Therefore, a second field interaction only can bring more amplitude up, creating population in the excited state, and it cannot bring the amplitude from the first field interaction back down to the ground electronic state S_0. In contrast, if the pulse frequency corresponds to the $0\rightarrow0$ transition, a second field interaction can bring the amplitude from the first field interaction back down to S_0, creating a displaced hole in the ground electronic state. Hence an excitation in the range of the $0\rightarrow1$ transition creates a nonstationary excited state component, while an excitation in the range of the $0\rightarrow0$ transition discriminates against it.

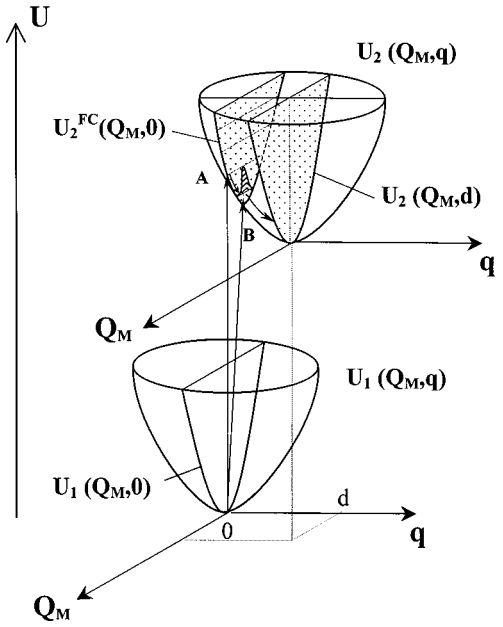

FIG. 11. The picture of two-dimensional potentials. Q_M is the coordinate of the OAHF intramolecular vibration.

Thus, the effect of OAHF intramolecular modes strongly depends on the carrier pulse frequency ω.

IV. CONCLUSION

In this work we have studied the effect of HF intramolecular modes on the chirped pulse excitation in condensed phase. The problem was solved using the double-sided Feynman diagrams.[36–38] We have shown that the application of the double-sided Feynman diagrams to systems with fast electronic dephasing opens up new possibilities for using this technique in resonance nonlinear optical spectroscopy. The novel potentials are including strong system–bath interactions (non-Markovian relaxation) and the summation of diagrams.

We have formulated the diagrammatic technique for fast optical dephasing by the partial summation of definite diagrams and then carried out a total diagram summation. The partial summation of diagrams is carried out by introducing the rectangular vertices, which are the sums of two subdiagrams corresponding to the nondiagonal density matrix elements in technique.[36] Introducing such vertices strongly diminishes a number of the diagrams under consideration.

In our technique the system evolution depends only on even times (see Sec. II D). The similar approximation of very fast dephasing during odd time periods was used by Mukamel, Yan, and Sparpaglione in their works on electronic transfer rates to sum an infinite series.[62,63]

Damping in our technique is included as a random perturbation by a Markovian process in the relevant electronic state. As this takes place, the relaxation itself is not Markovian since a system–bath interaction can be strong. A Markovian nature of a random perturbation enables us to write easily an expression for the corresponding diagram in any order with respect to the light–matter interaction.

Furthermore, only three types of the rectangular vertices exist. This point enables us to make the graphical summation of diagrams. To our knowledge, it is the first graphical summation of double-sided Feynman diagrams in literature. The last procedures has enabled us to obtain nonperturbative equations for the populations of molecular electronic states under the action of intense chirped pulses in the presence of HF quantum modes.

Using these equations, we have studied the influence of the chirp rate on the excited-state population n_2 after the completion of pulse action. We have shown that the effect of the OAHF intramolecular modes strongly depends on the carrier pulse frequency. Incorporating the intramolecular modes increases n_2 when a molecule is excited near the $0 \rightarrow 1$ transition with respect to the OAHF vibration. If the molecule is excited near the $0 \rightarrow 0$ transition with respect to the OAHF intramolecular mode, the effect is opposite. These results are explained by the picture of two-dimensional potentials corresponding to the OA HF and LF vibrations.

Finally, the absorption spectrum of large molecules in solutions is directly related to the vibrationally nonequilibrium populations in the ground and excited electronic states, when measured using high-power and comparative strongly chirped pulses.[64] These populations can be obtained by the solution of Eq. (42). The effect of the OAHF intramolecular modes on the absorption spectrum of an intense chirped pulse will be studied elsewhere.

ACKNOWLEDGMENTS

All the numerical calculations were performed using the SSDP-2 software package developed by E. Krissinel and N. Agmon.[65] This work was supported by Ministry of Absorption of Israel.

[1] B. Amstrup *et al.*, Phys. Rev. A **48**, 3830 (1993).
[2] B. Amstrup, G. Szabo, R. A. Sauerbrey, and A. Lorincz, Chem. Phys. **188**, 87 (1994).
[3] A. Poloviita, K. A. Suominen, and S. Stenholm, J. Phys. B **28**, 1463 (1995).
[4] S. Ruhman and R. Kosloff, J. Opt. Soc. Am. B **83**, 5013 (1990).
[5] B. Kohler *et al.*, Phys. Rev. Lett. **74**, 3360 (1995).
[6] J. S. Melinger, A. Hariharan, S. R. Gandhy, and W. S. Warren, J. Chem. Phys. **95**, 2210 (1991).
[7] J. S. Melinger *et al.*, J. Chem. Phys. **101**, 6439 (1994).
[8] C. J. Bardeen, Q. Wang, and C. V. Shank, Phys. Rev. Lett. **75**, 3410 (1995).
[9] E. T. J. Nibbering, D. A. Wiersma, and K. Duppen, Phys. Rev. Lett. **68**, 514 (1992).
[10] K. Duppen, F. de Haan, E. T. J. Nibbering, and D. A. Wiersma, Phys. Rev. A **47**, 5120 (1993).
[11] M. Sterling, R. Zadoyan, and V. A. Apkarian, J. Chem. Phys. **104**, 6497 (1996).
[12] E. M. Hiller and J. A. Cina, J. Chem. Phys. **105**, 3419 (1996).
[13] G. Cerullo, C. J. Bardeen, Q. Wang, and C. V. Shank, Chem. Phys. Lett. **262**, 362 (1996).
[14] C. J. Bardeen, Q. Wang, and C. V. Shank, J. Phys. Chem. A **102**, 2759 (1998).
[15] A. H. Buist *et al.*, Opt. Lett. **24**, 244 (1999).
[16] D. Huppert, B. D. Fainberg, and J. Segal, *Abstracts of the 6th French–Israeli Symposium on Nonlinear and Quantum Optics* (Les Houches, 2000), pp. Mo–P14.
[17] J. L. Krause *et al.*, J. Chem. Phys. **99**, 6562 (1993).
[18] B. D. Fainberg, Opt. Spectrosc. **67**, 137 (1989) [Opt. Spektrosk., V. **67**, 241 (1989)].
[19] B. D. Fainberg, Chem. Phys. **148**, 33 (1990).
[20] L. Seidner, G. Stock, and W. Domcke, J. Chem. Phys. **103**, 3998 (1995).
[21] S. Guerin, Phys. Rev. A **56**, 1458 (1997).
[22] Y. Tanimura and S. Mukamel, J. Phys. Soc. Jpn. **63**, 66 (1994).
[23] D. H. Schirrmeister and V. May, Chem. Phys. **220**, 1 (1997).
[24] B. D. Fainberg, J. Chem. Phys. **109**, 4523 (1998).
[25] C. J. Bardeen, J. Cao, F. L. H. Brown, and K. R. Wilson, Chem. Phys. Lett. **302**, 405 (1999).
[26] B. D. Fainberg and V. Narbaev, J. Mol. Liq. **86**, 201 (2000).
[27] C. J. Bardeen and C. V. Shank, Chem. Phys. Lett. **226**, 310 (1994).
[28] B. D. Fainberg, in *Advances in Multiphoton Processes and Spectroscopy*, edited by S. H. Lin, A. A. Villaeys, and Y. Fujimura (World Scientific, Singapore, New Jersey, London, in press).
[29] A. B. Gelman, Theor. Exp. Chem. **19**, 256 (1983) [Teoret. Eksperim. Khimiya **19**, 281 (1983)].
[30] J. Jortner and M. Bixon, J. Chem. Phys. **88**, 167 (1988).
[31] A. I. Burshtein, P. A. Frantsuzov, and A. A. Zharikov, J. Chem. Phys. **96**, 4261 (1992).
[32] R. A. Marcus, J. Chem. Phys. **24**, 966 (1956).
[33] L. D. Zusman, Chem. Phys. **49**, 295 (1980).
[34] J. T. Hynes, J. Phys. Chem. **90**, 3701 (1986).
[35] I. Rips and J. Jortner, J. Chem. Phys. **87**, 6513 (1987).
[36] T. K. Yee and T. K. Gustafson, Phys. Rev. A **18**, 1597 (1978).
[37] M. Aihara, Phys. Rev. A **18**, 606 (1978).
[38] J. P. Uyemura, IEEE J. Quantum Electron. **QE-16**, 472 (1980).
[39] B. D. Fainberg, J. Chin. Chem. Soc. **47**, 579 (2000).
[40] Y. R. Shen, *The Principles of Nonlinear Optics* (Wiley, New York, 1984).
[41] S. Mukamel, *Principles of Nonlinear Optical Spectroscopy* (Oxford University Press, New York, 1995).
[42] M. Lax, J. Chem. Phys. **20**, 1752 (1952).
[43] B. I. Yakobson and A. I. Burshtein, Chem. Phys. **49**, 385 (1980).
[44] W. Jarzeba *et al.*, J. Phys. Chem. **92**, 7039 (1988).
[45] V. L. Bogdanov and V. P. Klochkov, Opt. Spectrosc. **44**, 412 (1978).
[46] V. L. Bogdanov and V. P. Klochkov, Opt. Spectrosc. **45**, 51 (1978).
[47] V. L. Bogdanov and V. P. Klochkov, Opt. Spectrosc. **52**, 41 (1982).
[48] S. Y. Goldberg *et al.*, Chem. Phys. **183**, 217 (1994).
[49] M. L. Horng, J. Gardecki, A. Papazyan, and M. Maroncelli, J. Phys. Chem. **99**, 17311 (1995).
[50] T. Joo *et al.*, J. Chem. Phys. **104**, 6089 (1996).
[51] E. Wigner, Phys. Rev. **40**, 749 (1932).
[52] M. Hillery, R. F. O'Connel, M. O. Scully, and E. P. Wigner, Phys. Rep. **106**, 121 (1984).
[53] D. Y. Yang and S. Y. Sheu, J. Chem. Phys. **106**, 9427 (1997).
[54] R. Kubo and Y. Toyozawa, Prog. Theor. Phys. **13**, 160 (1955).
[55] H. Mori, Prog. Theor. Phys. **34**, 399 (1965).
[56] J. M. Deutch and I. Oppenheim, J. Chem. Phys. **54**, 3547 (1971).
[57] A. O. Caldeira and A. J. Leggett, Physica A **121**, 587 (1983).
[58] Y. J. Yan and S. Mukamel, J. Chem. Phys. **89**, 5160 (1988).
[59] R. S. Fee and M. Maroncelli, Chem. Phys. **183**, 235 (1994).
[60] S. H. Lin, Theor. Chim. Acta **10**, 301 (1968).
[61] M. Abramowitz and I. Stegun, *Handbook on Mathematical Functions* (Dover, New York, 1964).
[62] M. Sparpaglione and S. Mukamel, J. Chem. Phys. **88**, 3263 (1988).
[63] S. Mukamel and Y. J. Yan, Acc. Chem. Res. **22**, 301 (1989).
[64] B. D. Fainberg, Chem. Phys. Lett. (to be published).
[65] E. B. Krissinel and N. Agmon, J. Comput. Chem. **17**, 1085 (1996).